Tribology International 186 (2023) 108604

Contents lists available at ScienceDirect

Tribology International

journal homepage: www.elsevier.com/locate/triboint

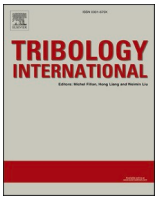

Investigating the effect of novel self-lubricant TiSiVN films on topography, diffusion and oxidation phenomenon at the chip-tool interface during dry machining of Ti-6Al-4V alloy

Ch Sateesh Kumar [a,b], Gorka Urbikain [a,b,*], Luis Norberto López de Lacalle [a,b], Soumya Gangopadhyay [c], Filipe Fernandes [d,e]

[a] CFAA, Aeronautics Advanced Manufacturing Center, University of the Basque Country (UPV/EHU), Biscay Science and Technology Park, Ed. 202, Zamudio, Spain
[b] Department of Mechanical Engineering, University of the Basque Country, Escuela Superior de Ingenieros Alameda de Urquijo S/N, 48013 Bilbao, Spain
[c] Department of Mechanical Engineering, Indian Institute of Technology, Bhilai, Raipur, 492015, Chhattisgarh, India
[d] University of Coimbra, CEMMPRE, ARISE, Department of Mechanical Engineering, Rua Luís Reis Santos, 3030-788 Coimbra, Portugal
[e] ISEP, Polytechnic of Porto, Rua Dr. António Bernardino de Almeida, 4249-015Porto, Portugal

ARTICLE INFO

Keywords:
TiSiVN
self-lubricating coating
surface roughness
Ti-6Al-4V
machining

ABSTRACT

Machining of titanium alloys such as Ti-6Al-4 V can be very intimidating due to their low thermal conductivity leading to elevated cutting temperatures at the chip-tool interface (I_{CT}). In this regard, the self-lubrication effect of coatings like TiSiVN represented by topography, oxidation, and diffusion at the chip-tool interface are crucial. Thus, the present work investigates the latter three mechanisms during dry machining of Ti-6Al-4 V titanium alloy with uncoated and TiSiVN coated Al_2O_3/SiC whiskers-reinforced ceramic cutting tools. The results reveal that the adhesion height (*AH*) and O% increases with cutting temperature, showing the dominant influence of cutting temperature on material adhesion and oxidation levels at the I_{CT}. AH increases with increased cutting speed for both coated tools, indicating that the crater depth increment was not so severe for the coated tools. However, a drastic upward surge of crater depth for uncoated and TiSiN coated tools at 125 m/min cutting speed makes the crater edge near the I_{CT} act as a chip breaker and facilitates the chip's bending away from the tool face causing reduction in chip bend angles (*BA*). Additionally, the TiSiVN coating accounts to a reduction of approximately 23% in *AH* and 18% in *Ti%, and 37%* lower oxygen levels at the highest cutting speed when compared to the uncoated tool primarily due to lower cutting temperatures and self-lubricating behavior.

1. Introduction

Titanium alloys owing to their favorable material properties such as high strength-to-weight ratio, toughness, superb corrosion resistance, and bio-compatibility, find their application in the automobile, aerospace, and medical industries [1]. However, their low thermal conductivity, work-hardening capability during machining, and high chemical reactivity at temperatures above 500 °C categorize them as extremely difficult-to-cut [2,3]. The lower thermal conductivity would prevent heat dissipation through the chips generated during machining, leading to extreme temperatures at the chip-tool interface causing high tool wear [4]. Further, during the machining of titanium alloys, due to the above-discussed problems, cutting tools go through wear mechanisms such as diffusion, attrition, adhesion, seizure, and abrasion [5,6]. Also, the higher tendency of chemical reactivity for titanium alloys at elevated temperatures causes a drastic increase in tool wear, thus limiting the machining of titanium alloys at lower cutting speeds.

Researchers around the globe are primarily focused on investigating the wear mechanism and improving the tool life of cutting tools during the machining of titanium alloys. In this regard, Lindvall et al. [7]

Abbreviations: Ø,, Chip bend angle; *AH,*, Adhesion height; C_{HI},, Crater height at chip-tool interface; I_{CT},, Chip-tool interface; *EDS,*, Energy dispersive spectroscopy; *FESEM,*, Field emission scanning electron microscope; *KT,*, Maximum crater depth; *O%,*, Oxygen percentage; *MQL,*, Minimum quantity lubrication; *PCBN,*, Polycrystalline cubic boron nitride; *PCD,*, Polycrystalline diamond; *Ra,*, Average surface roughness at the chip-tool interface; R_Z,, Maximum peak to valley height at the chip-tool interface; *Ti%,*, Titanium percentage.

* Corresponding author at: CFAA, Aeronautics Advanced Manufacturing Center, University of the Basque Country (UPV/EHU), Biscay Science and Technology Park, Ed. 202, Zamudio, Spain.
E-mail address: gorka.urbikain@ehu.eus (G. Urbikain).

https://doi.org/10.1016/j.triboint.2023.108604
Received 17 April 2023; Received in revised form 11 May 2023; Accepted 14 May 2023
Available online 15 May 2023

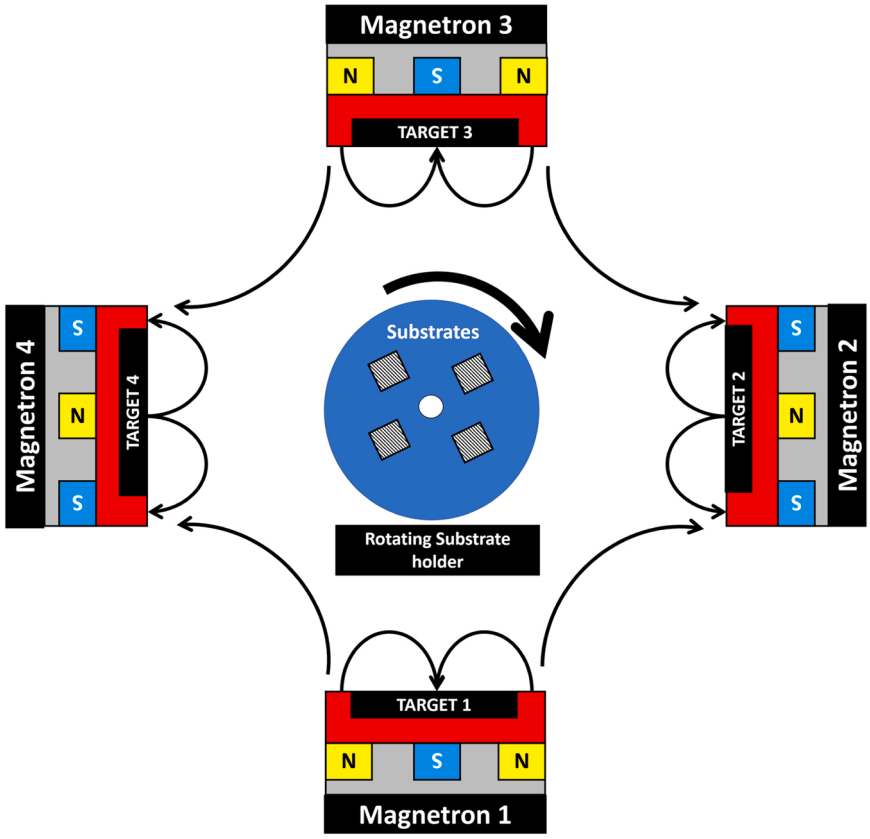

Fig. 1. Schematic representation of the DC reactive magnetron sputtering process.

Table 1
EDS elemental composition of as-deposited coatings and Ti-6Al-4 V titanium alloy.

Element	Percentage composition (at%)		
	Coating		Workpiece material
	TiSiN	TiSiVN	Ti-6Al-4 V alloy
Ti	41.2 ± 0.8	33.9 ± 0.6	89.6 ± 0.4
Si	5.7 ± 0.2	5.3 ± 0.2	0
V	0	7.8 ± 0.3	4.2 ± 0.15
N	52.1 ± 1.1	51.3 ± 1.2	0
O	0.6 ± 0.1	1.4 ± 0.1	0.1 ± 0.05
Al	0	0	6.1 ± 0.2

Table 2
Mechanical and thermal properties of Ti-6Al-4 V titanium alloy [34].

Property (Unit)	Value
Density (kg/m^3)	4430
Yield strength (MPa)	880
Ultimate tensile strength (MPa)	950
Thermal conductivity (W/mK)	17
Elastic modulus (GPa)	113.8
Poisson's ratio	0.342
Heat capacity (J/kgK)	526

presented polycrystalline diamond (*PCD*) and polycrystalline cubic boron nitride (PCBN) tools as a sustainable replacement for cemented carbide tools and revealed that tool-protective layers were formed as a result of a reaction between tool and workpiece material. Also, it has been reported that alumina based mixed ceramic tools with reinforcements like SiC whiskers owing to their superior fracture toughness and thermal shock resistance [8], can be an effective and economical alternative to costly PCBN and PCD cutting tools [9,10]. Further, the literature suggests that the use of lubrication or coolants can be an effective way of reducing tool wear during machining difficult-to-cut materials [11–15]. When considering titanium alloys, using minimum quantity lubrication (MQL) and graphene-based nano-fluid during machining Ti-6Al-4 V alloy helped to enhance the machining performance by generating superior surface quality of the machined surface. Also, it accounted for a lower friction coefficient when compared to the dry state [16]. Gupta et al. [17] studied the application of hybrid cryo-lubrication during turning of Ti-6Al-4 V alloy and reported significant reduction in tool wear. Further, Eltaggaz et al. [18] revealed that integration of nanofluids with conventional MQL techniques accounted to lower chip-tool contact lengths and adhesion levels. Similarly, many studies reveal the effectiveness of lubrication and cooling during the machining of titanium alloys [3,19–21].

Further, thin-film depositions on the cutting tools such as hard coatings like AlTiN, AlCrN, TiN, and low friction coatings like DLC, WC/C can also be an effective way of improving the cutting tool durability [22–28]. There is another class of coatings termed self-lubricating coatings that generate lubricious phases during machining that act as friction-reducing agents during the machining process [29]. Mainly, adding vanadium to transition metal nitrides such as AlCrSiN and TiSiN causes rapid oxidation at elevated temperatures leading to the formation of V_nO_{3n-1} low melting point lubricious phases resulting in the reduction of coefficient of friction [30,31]. However, not much work has been carried out on the application of vanadium-based self-lubricating coatings during the machining of titanium alloys. The deposited thin-films act as a protective thermal barrier and prevent heat at the chip-tool interface by reaching the tool core due to the formation of tribolayer [32].

Further, exploration of the chip-tool interface is a significant part of tool wear analysis due to the movement of the chip over the tool face

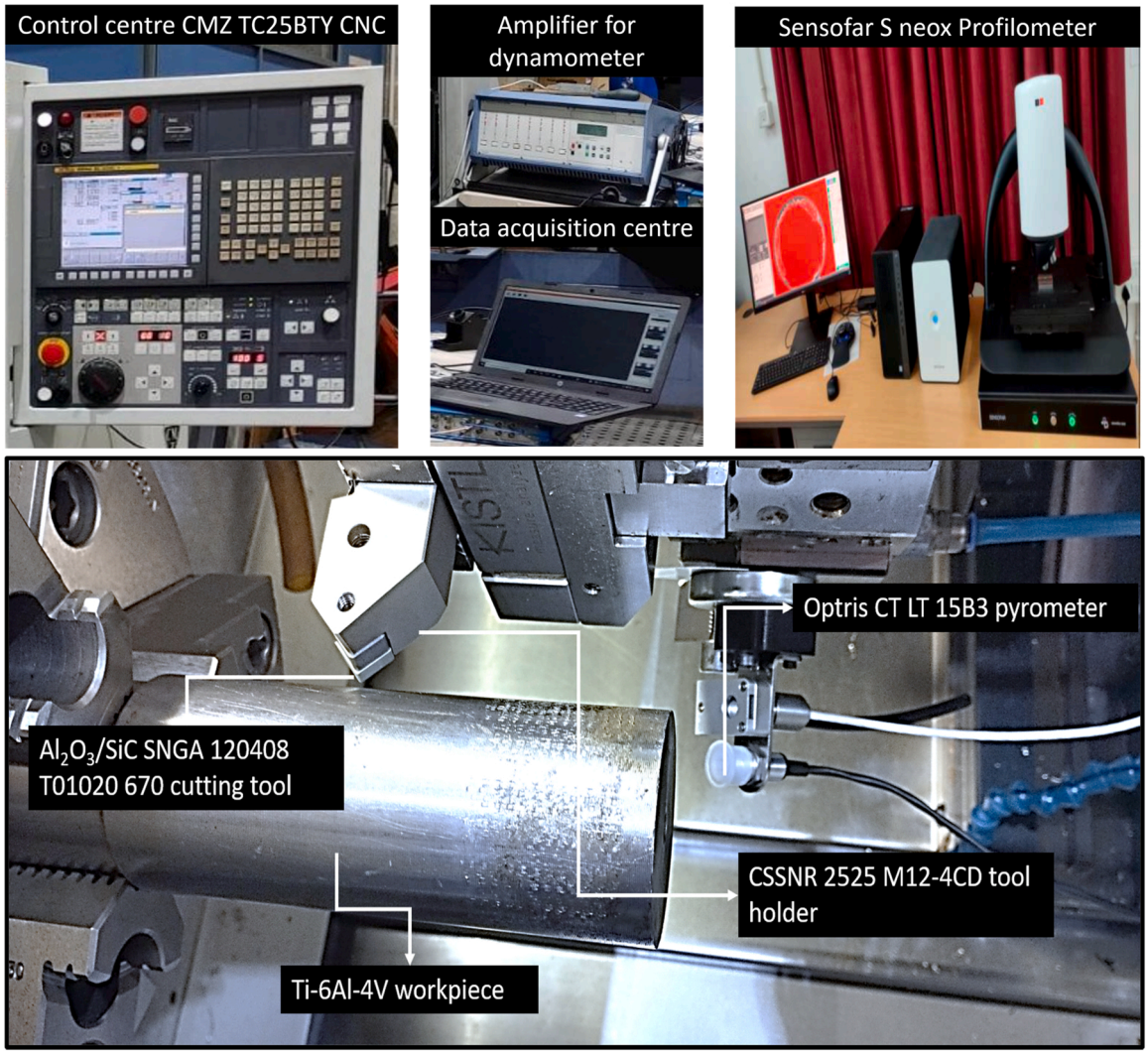

Fig. 2. Experimental setup for dry turning of Ti-6Al-4 V titanium alloy.

Table 3
Dry turning test parameters for Ti-6Al-4 V alloy.

Cutting speed (in m/min)	50, 75, 100, 125
Feed rate (in mm/rev)	0.1
Depth of cut (in mm)	0.5
Coatings	TiSiN, TiSiVN
Cutting tool	SNGN 120408 T01020 Al_2O_3/SiC ceramic cutting tools
Workpiece	Ti-6Al-4 V titanium alloy
Tool holder	CSSNR 2525 M12–4CD

causing seizure, attrition, and abrasion [33]. However, not much work can be seen that provides a comprehensive investigation influencing the effect of self-lubricating coatings on chip-tool interface topography. This investigation becomes highly significant during the machining of titanium alloys, where chemical reactivity is very severe at higher cutting temperatures.

From the literature, it is evident that most researchers are concerned about tool wear and surface integrity during the machining of titanium alloys and provide possible solutions like lubrication, cooling, thin-film depositions for reducing tool wear, improving tool durability, and surface integrity of the machined surface. However, not much work is targeted on the topography and wear behavior exclusively at the chip-tool interface, which becomes very significant while machining titanium alloys due to heat accumulation at the chip-tool interface as a result of their low thermal conductivity. Thus, in the present work, the topography and wear behavior (diffusion and oxidation) at the chip-tool interface during dry turning of Ti-6Al-4 V titanium alloy with uncoated and TiSiVN coated Al_2O_3/SiC whiskers reinforced ceramic cutting tools will be investigated. TiSiN coating would also be deposited on the ceramic substrates which will be used as a reference for understanding the effect of the self-lubricating behavior of TiSiVN coating.

2. Experimental methodology

2.1. Coating deposition

TiSiN and TiSiVN coatings were deposited using DC power supplies in a TEER sputtering machine. The chamber has four cathodes uniformly distributed in relation to the center gravity of the chamber. High-purity Ti, Si, and V targets were used on the depositions. Before the depositions, the chamber was evacuated to a pressure of $7.5 \times 10–6$ mbar. First, Al_2O_3/SiC whiskers reinforced ceramic cutting inserts from Sankvik were etched in an Ar atmosphere for 40 min, using a pulsed bias of 650 V and a frequency of 250 kHz. During the etching time, the pair of Ti targets were cleaned for 20 min, applying 1000 W at each one. Then, for another 20 min, the Si and V targets were cleaned by applying a power of 300 and 1000 W, respectively. The described process had a pair of shutters in front of each pair of targets while etching to avoid cross-contamination between the targets and the substrate. Fig. 1 shows the

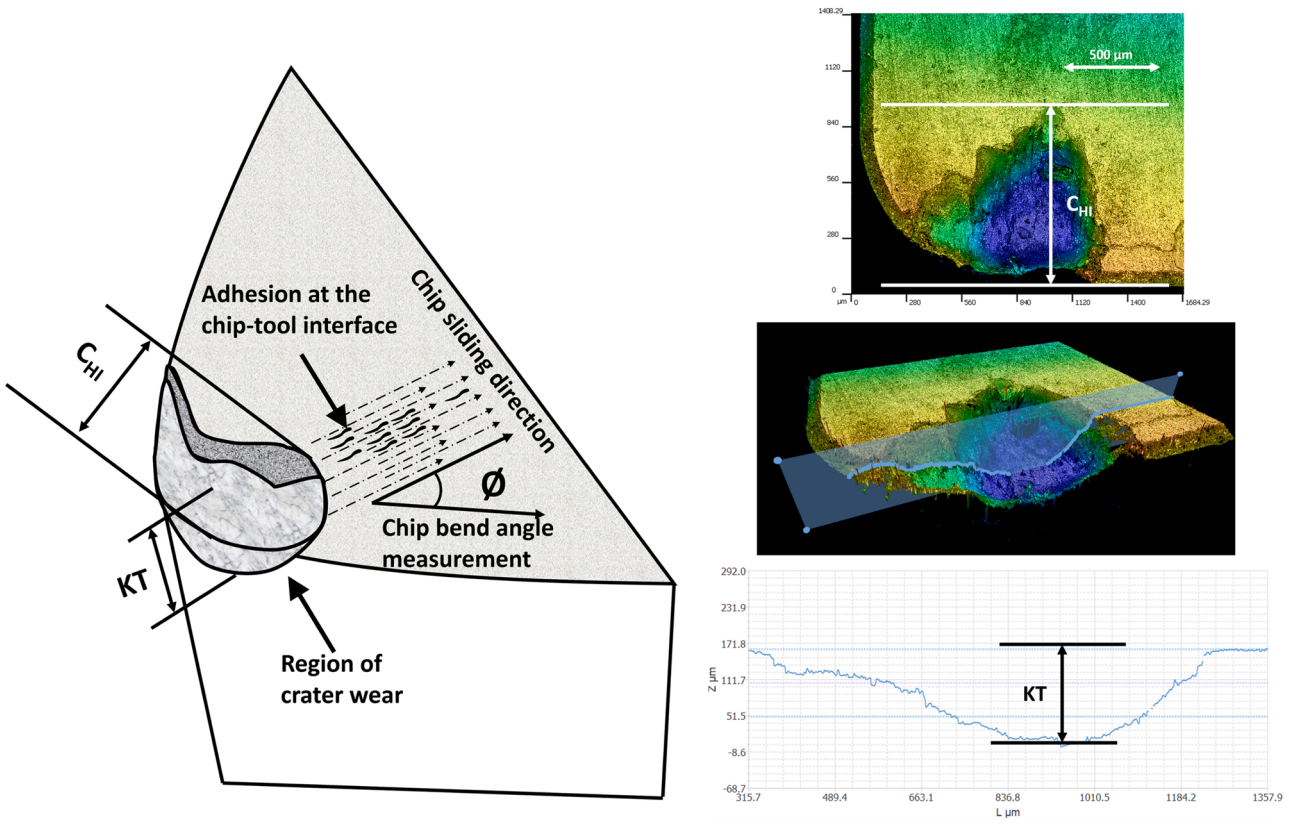

Fig. 3. Schematic representation of the chip-tool interface and different topography measurements.

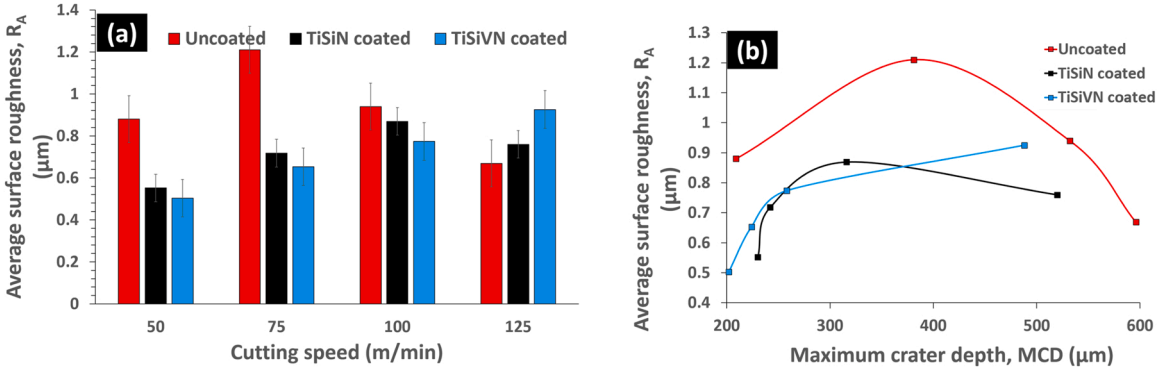

Fig. 4. Variation of (a) average surface roughness, *Ra* with cutting speed, and (b) average surface roughness, *Ra* with maximum crater depth, *KT*.

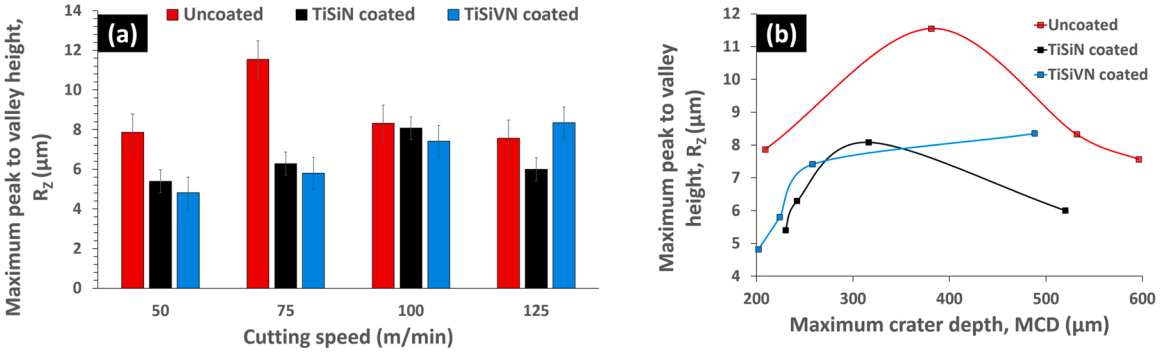

Fig. 5. Variation of (a) maximum peak to valley height, R_Z with cutting speed, and (b) maximum peak to valley height, R_Z with maximum crater depth, *KT*.

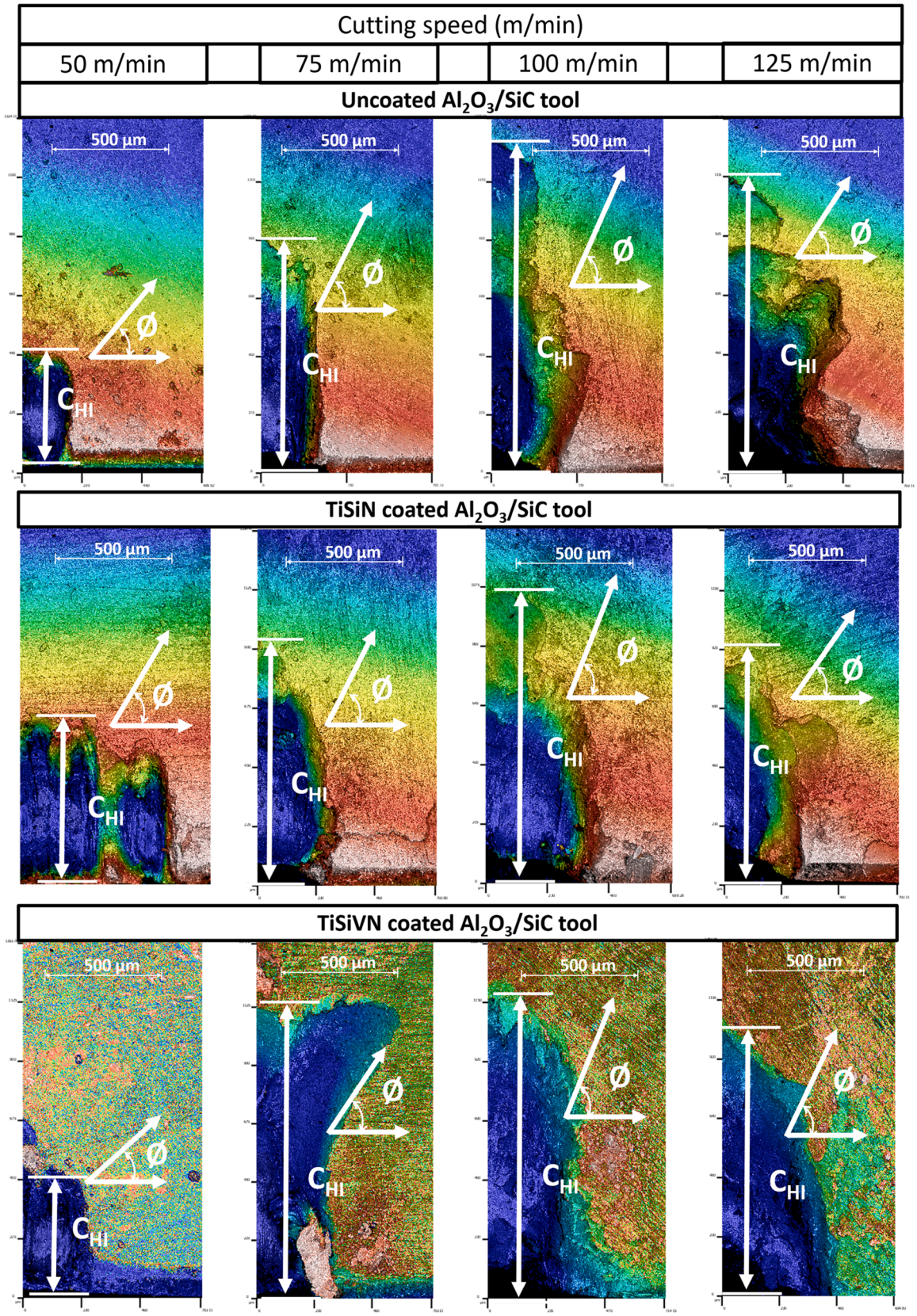

Fig. 6. 2D-profilometry images showing crater height (C_{HI}) and chip bend angle (Ø) in the I_{CT} for uncoated and coated Al_2O_3/SiC ceramic cutting tools at different cutting speeds.

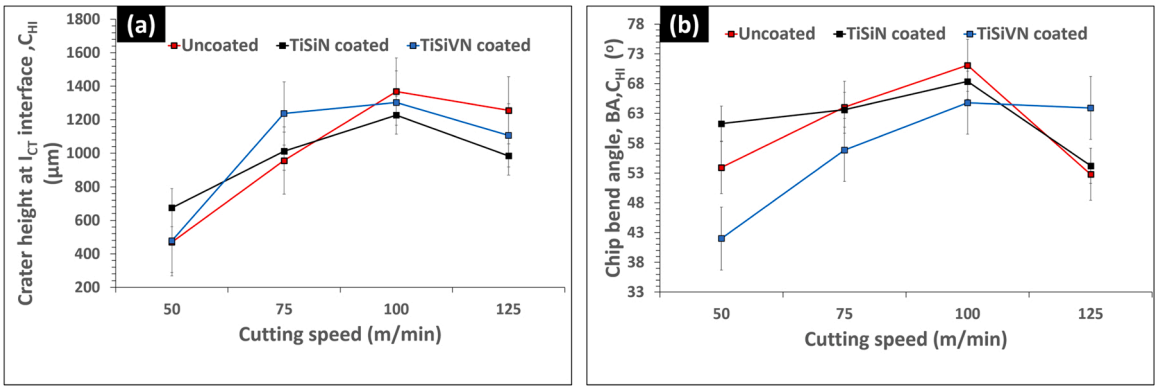

Fig. 7. Variation of (a) crater height, C_{HI}, and (b) chip bend angle, Ø with cutting speed for uncoated and coated cutting tools.

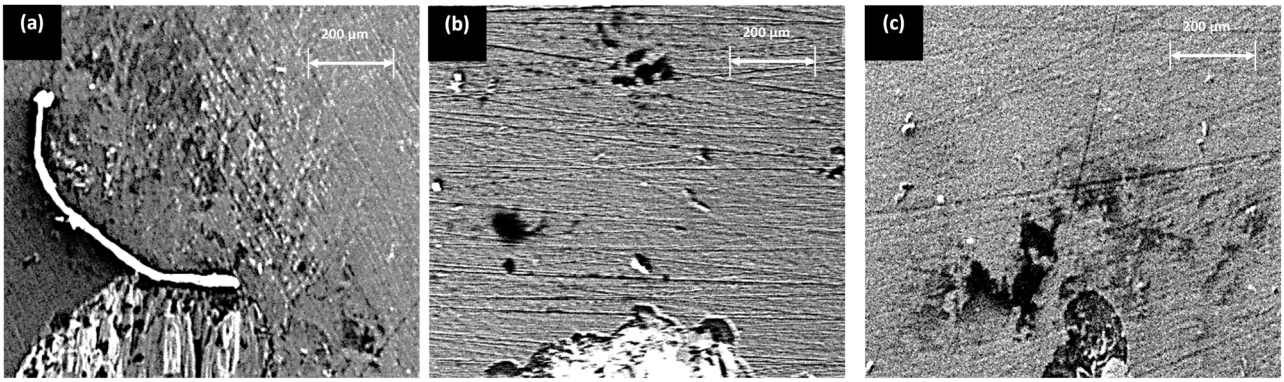

Fig. 8. SEM topography of the CI interface showing adhesion for (a) uncoated, (b) TiSiN coated, and (c) TiSiVN coated Al2O3/SiC ceramic cutting tool at 50 m/min cutting speed.

schematic representation of the coating process, whereas the elemental composition of the as-deposited coatings obtained from EDS spectroscopy has been listed in Table 1.

2.2. Machining tests and measurements

All the turning tests were performed on a CMZ TC25BTY CNC machine with 35 KW spindle power. The Al_2O_3/SiC whiskers reinforced ceramic cutting inserts with and without coating having designation SNGN 120408 T01020 670 (manufacturer: Sandvik Coromant) mounted on CSSNR 2525 M12–4CD tool holder (manufacturer: Sandvik Coromant) were used for the turning Ti-6Al-4 V titanium alloy under dry cutting environment. The mechanical and thermal properties of the workpiece material have been listed Table 2 whereas the EDS elemental composition has been shown in Table 1. The experimental setup for the turning tests has been shown in Fig. 2. The cutting speed was varied between 50 and 125 m/min with an interval of 25 m/min while keeping the feed rate and depth of cut constant at 0.1 mm/rev and 0.5 mm, respectively. The machining test parameters are shown in Table 3. The cutting parameters have been selected based on the recommendation of the tool manufacturer. However, higher cutting speeds are considered to explore the improvement offered by the TiSiVN coated tool over uncoated cutting tool. A 100 mm continuous cut was done for each test with each repeated thrice to keep the machining errors at minimum. CT LT 15B3 non-contact pyrometer was used to make the temperature measurements during the machining process. The pyrometer is equipped with the manufacturer supplied Optris Compact Connect software for the visualization of measurements. The instrument has a fast response time of 150 ms and an accuracy of ± 1 °C. The cutting temperature was measured by pointing the pyrometer at the cutting zone and a continuous measurement was made over the length of cut. An average of the measured temperature was considered as the final reading.

After the tests, the topography of the chip-tool interface was explored using Sensofar 2D profilometer (model: S neox). The schematic representation of the region under consideration and different measurements on the chip-tool interface are shown in Fig. 3. The chip-bend angles are measured by identifying the chip sliding marks on the tool rake surface. The direction of chip bending is considered in relation to the major cutting edge of the insert. The tool wear and oxidation studies were carried out using Carl Zeiss make (model: GEMINI SEM 500 KMAT) field-emission scanning electron microscope (FESEM) equipped with energy dispersive spectroscopy (EDS). Raman spectroscopy analyses were conducted, too, to characterize some oxides. The topography evaluation was carried out using Sensoview software with version 1.6.0.

3. Results and discussion

3.1. Profilometry at chip-tool interface

Fig. 4(a) shows the variation of average surface roughness, *Ra* at the chip-tool interface (I_{CT}) with cutting speed for uncoated and coated Al_2O_3/SiC ceramic cutting tools. It is observed that *Ra* at the I_{CT} increase for the uncoated tool when the cutting speed increases to 75 m/min. However, any further increase in cutting speed causes a reduction of *Ra*. Whereas, for TiSiN coated tool the *Ra* increases till 100 m/min cutting speed and then decreases slightly at 125 m/min.

On the contrary, for TiSiVN coated tool *Ra* increases with cutting speed till 125 m/min. This behavior of surface roughness at the I_{CT} is further investigated by plotting *Ra* against maximum crater depth, *KT*, in Fig. 4(b). *KT* increases drastically when the cutting speed increases for uncoated cutting tools, whereas for TiSiN and TiSiVN coated tools, the increase in *KT* with cutting speed was much more gradual till 100 m/

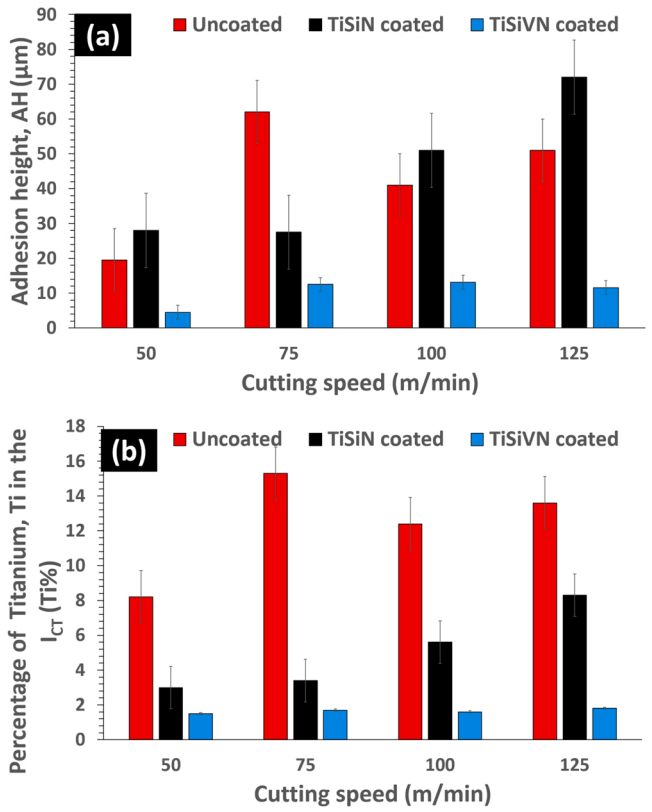

Fig. 9. Variation of (a) adhesion height, *AH*, and (b) *Ti%* in the I_{CT} with cutting speed for uncoated and coated cutting tools.

min cutting speed and then a sudden increase in *KT* was noted at 125 m/min cutting speed. The increased crater depth can be directly related to the wear resistance of cutting tools with higher *KT* corresponding to higher tool wear. However, increasing crater depth at some point should cause loss of effective cutting edge and increase the crate width with the increase of cutting speed. These complex phenomena can further be co-related to the roughness at the I_{CT}. The decrease in *Ra* can be attributed to the uncoated cutting tool's loss of effective cutting edge at higher cutting speeds. A similar trend can be seen for both uncoated and coated cutting tools for the maximum peak-to-valley height, R_Z at the I_{CT} (see Fig. 5(a) and 5(b)). The coated tools offer lower surface roughness at the I_{CT} except at 125 m/min cutting speed. The TiSiN coated tool corresponds to the lowest values of *Ra* till 100 m/min cutting speed. The higher roughness for coated tools at 125 m/min cutting speed requires further investigation.

From the above discussion, it is evident that the crater depth has a significant impact on the roughness at the I_{CT}, and also it is inevitable to understand the chip flow over the tool face to comprehend the effect of chip movement over the tool rake face with the subsequent adhesion at the I_{CT}. In this regard, Fig. 6 shows the variation of cater height, $C_{HI,}$ and chip bend angle, Ø at I_{CT} with cutting speed for uncoated and coated tools. Also, the measured values of C_{HI} and Ø have been plotted against cutting speed in Fig. 7. The crater moves inside the I_{CT} in terms of width and height with the growing cutting speed. A drastic upward surge of crater depth makes the crater edge near the I_{CT} act as a chip breaker and facilitates the chip's bending away from the tool face. Thus, the chip bend angle reduces at the highest cutting speed of 125 m/min for the uncoated and TiSiN coated tool.

On the contrary, for TiSiVN coated tool, the *KT* is much lower when compared to the other tools, and thus, the chip bending is not so prominent. However, the increase in Ø with cutting speed for the self-lubricating TiSiVN coated tool is very low at 125 m/min, basically due to the drastic increase of crater depth compared to that at 100 m/min cutting speed. The upsurge in Ø with cutting speed is fundamentally due to C_{HI} penetration into the I_{CT} with the increase in cutting speed. The lower penetration of C_{HI} for TiSiN and TiSiVN coated tools at higher cutting speeds (i.e., at 100 m/min and 125 m/min) in comparison to uncoated tools exhibits superior wear resistance for coatings with TiSiVN coating outperforming the TiSiN coating mainly due to its self-lubricating properties which will be discussed later.

3.2. Adhesion behavior at chip-tool interface

Another critical phenomenon at the I_{CT} is seizure due to the adhesion of the moving chips. Fig. 8 shows the adhesion behavior for uncoated, TiSiN coated, and TiSiVN coated Al_2O_3/SiC whiskers reinforced ceramic cutting tools during dry machining of Ti-6Al-4 V titanium alloy at 50 m/min cutting speed. At this lower cutting speed, both TiSiN and TiSiVN coatings exhibit superior anti-adhesive properties with low levels of material adhesion when compared to the uncoated tool. Also, the chip sliding marks were prominent on all the surfaces with TiSiVN coating showing excellent resistance to sliding basically due to lower seizure levels and self-lubricating properties of the coating. However, understanding the adhesion at the I_{CT} as a function of cutting speed is necessary to get an apparent perception of the effect of crater height, $C_{HI,}$ and cutting temperature on the adhesion behavior. In this regard, Fig. 9 (a) shows the variation of adhesion height, *AH* with cutting speed for uncoated and coated tools, respectively. *AH* grows drastically for the uncoated tool when the cutting speed increases to 75 m/min and then falls from its maximum value. The severe crater depth increment for the uncoated tool at higher cutting speeds in combination with high chip flow velocity due to the increase of cutting speed should bend the chips away from the tool face [35] resulting in lower adhesion at the I_{CT}. On the contrary, for both coated tools, *AH* increases with the growth of cutting speed, indicating that the crater depth increment was not so severe for coated tools. TiSiVN coated tool interestingly accounted for extremely low levels of *AH*.

Fig. 9(b) shows the percentage variation of titanium (*Ti%*) with cutting speed in the adhesion zones determined on the cutting tools. *Ti%* has been obtained by doing EDS on the adhesion region on the I_{CT} with no coating delamination to avoid interference of Ti present in the coatings on the readings. The *Ti%* on the I_{CT} follows the trend of *AH* variation with cutting speed for both uncoated and coated cutting tools. Also, it is interesting to note that the *Ti%* is higher for the uncoated tool when compared to TiSiN coated tool at 100 m/min and 125 m/min cutting speeds, which is mainly because of adversity of the crater depth for the uncoated tool at these cutting speeds causing higher chip bending accounting to lower values of Ø (see Fig. 7(b)). TiSiVN coated tool accounted for the lowest values of *Ti%* in the adhesion zones under all cutting conditions. Also, the roughness zones shown in Fig. 10 indicate that the adhesion shifts more towards the cutting edge with the increased cutting speed due to the increased crater depth for the uncoated tool. Further, abrasion can be seen on all the cutting tools with its direction following the chip bend angles. The TiSiVN coating shows signs of lower abrasion compared to TiSiN-coated and uncoated tools, but coating delamination at the edges is observed, which is caused basically due to the movement of chips.

On the contrary, for the tool with TiSiN coating, the adhesion zone remains mostly towards the cutting edge, whereas for TiSiVN coated tool, no severe adhesion can be seen. Further, when the abrasion due to the movement of chips on the I_{CT} is considered, the TiSiVN coating successfully prevents the formation of severe abrasion on the coating compared to TiSiN coating. Also, on TiSiN coating, the prominent abrasion marks may lead to more contact time for the chips on the I_{CT} due to higher resistance to movement of chips causing high adhesion, which is evident by higher values of *AH* for TiSiN coated tool.

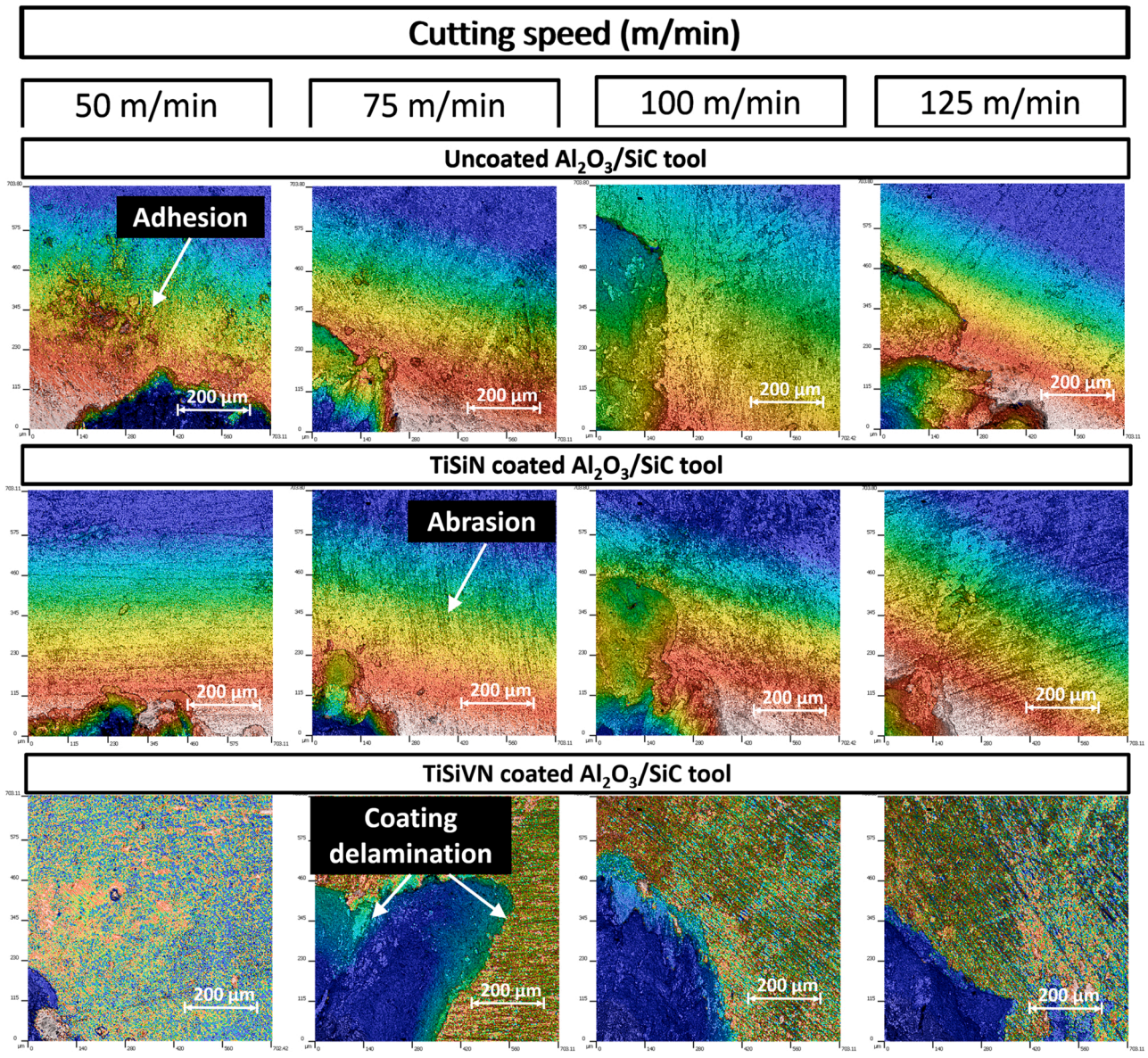

Fig. 10. 2D-profilometry roughness zone growth with cutting speed for uncoated and coated cutting tools.

3.3. Effect of temperature on topography at chip-tool interface

The heat generated during machining is one of the most critical factors affecting the I_{CT} topography behaviour. However, it has been reported by various researchers that an increase of cutting speed causes an increase in cutting temperatures [36–38] which is also observed in the present scenario. The coated tools tend to generate lower cutting temperatures with TiSiVN coating exhibiting superior performance. However, it is necessary to corelate cutting temperature with parameters at I_{CT} in the present investigation. In this regard, Fig. 11 shows the variation of chip bend angle (Ø), crater height (C_{HI}) and adhesion height (AH) at the I_{CT} with cutting temperature. Ø increases with cutting temperature for all cutting tools till 100 m/min cutting speed. At higher cutting temperatures, adhesion would be higher, which would restrict the movement of the chip in the I_{CT}. However, at 125 m/min cutting speed, the crater depth is the dominant parameter causing the bending of the chip away from the tool face resulting in lower chip bend angles. Further, similarly, C_{HI} decreases at 125 m/min cutting speed for all cutting tools after increasing with cutting speed till 100 m/min. The increase in temperature would cause more seizure levels and adhesion at the I_{CT}, which is evident from the $Ti\%$ and AH values (see Fig. 11(d)). Also, the variation of AH with cutting temperature clearly shows the dominant influence of cutting temperature on material adhesion at the I_{CT}. The TiSiVN coated tool exhibited low levels of adhesion and chip bending in comparison to TiSiN coated and uncoated tools even at high cutting temperatures basically due to i) generation of lower cutting temperatures as a result of self-lubricating and anti-adhesive properties and ii) formation of lower crater depth causing lower bending of chips.

3.4. Oxidation and diffusion wear

Another important phenomenon at the I_{CT} that can take place is the oxidation of the tool, workpiece, and coating material. In this regard, the oxygen percentage ($O\%$) has been plotted against cutting speed for uncoated and coated cutting tools in Fig. 12(a). Also, the variation of $O\%$ with cutting temperature has been shown in Fig. 12(b). The $O\%$ was considered only at the places of material adhesion or seizure to eliminate errors due to oxygen in the cutting tool material. The $O\%$ increases with the increment of cutting speed for all cutting tools. The TiSiVN coating accounts to lower oxygen levels at the I_{CT} owing to generation of lower

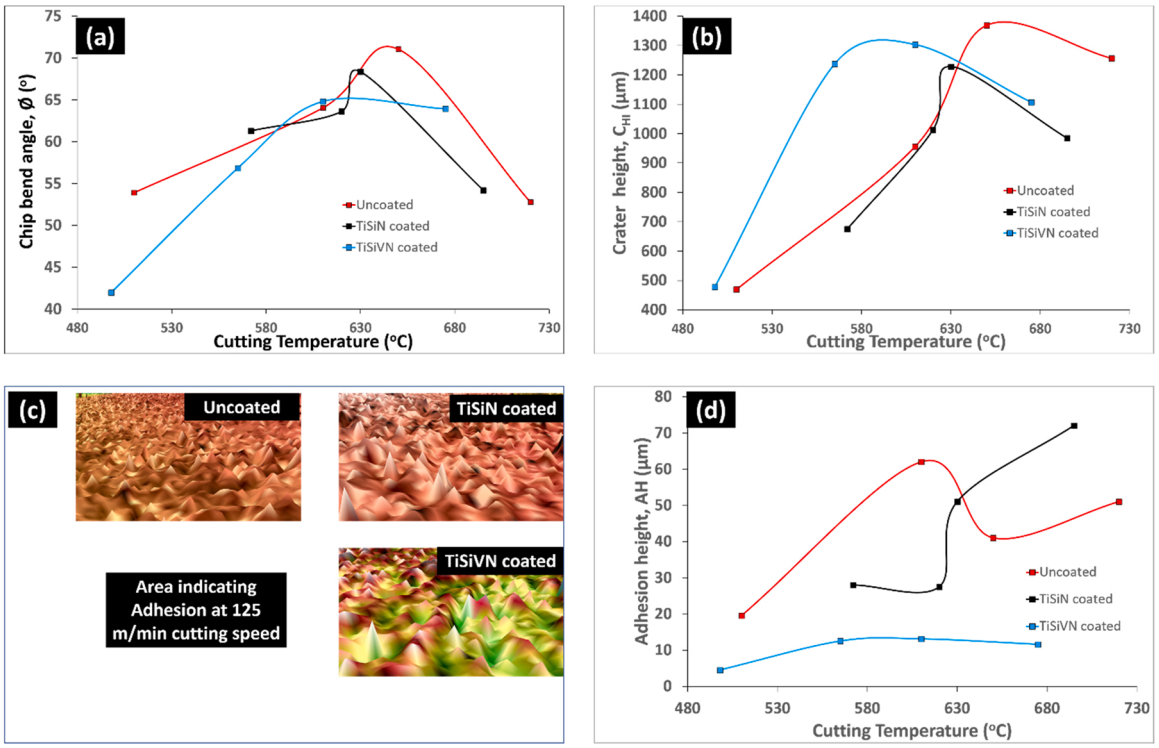

Fig. 11. Variation of (a) chip bend angle, Ø (b) crater height, C_{HI} and (d) adhesion height, *AH* with cutting temperature & (c) Area indicating adhesion at 125 m/min cutting speed.

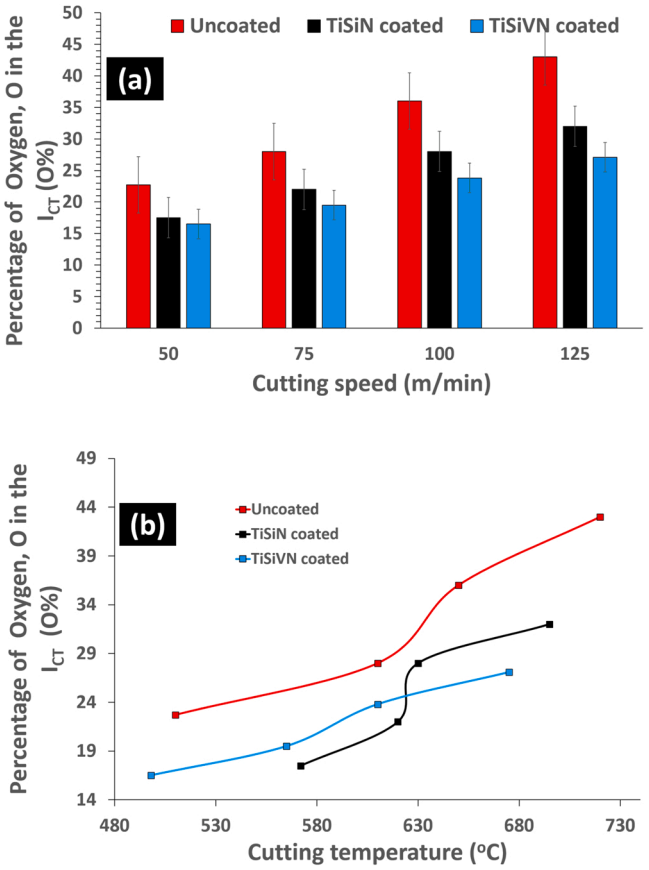

Fig. 12. Variation of *O%* in the I_{CT} with cutting speed for uncoated and coated cutting tools.

cutting temperatures which is followed by TiSiN coated and uncoated tool respectively. These results also indicate the dominant effect of cutting temperature on oxidation with higher cutting temperatures accounting to higher oxygen levels.

As per the above-discussed results, TiSiVN coating exhibits superior machining performance under all conditions, and thus, the self-lubricating behaviour of the TiSiN coating has been studied through elemental mapping (see Fig. 13), which may result in the reduction of friction at the I_{CT} and also lower abrasion on the flank face. The elemental mapping shown in Fig. 13 clearly shows the presence of oxygen along with vanadium, which is an indication of vanadium oxidation that is a necessary condition for forming V-O oxides [39,40]. These oxides form a tribolayer reducing friction [30] not only at the I_{CT} but also at sliding contact of the flank-workpiece interface, reducing erosion of the tool flank. Raman analysis conducted at such debris (see Fig. 14), indicates the presence of different oxides: rutile – TiO_2, V_2O_5, and SiO_2, in good agreement with the film chemical composition. The presence of V_2O_5 on the contact reduces friction [24] not only at the I_{CT} but also at the sliding contact of the flank-workpiece interface, thus reducing erosion on that zone.

It has been reported by Dearnley and Grearson [41] that temperatures above 800 °C initiate diffusion during the machining of Ti-6Al-4 V titanium alloy. However, it is near to impossible to explore the I_{CT} for temperature measurement; the measured temperatures are mostly the average in the chips. Also, the chip temperature is always 20–30% lower than that of the interface temperature [42]. Thus, it can be assumed that the exact interface temperature is much higher than that reported in Fig. 11. Further, alumina-based ceramic tools provide better resistance to thermal deterioration of the cutting tools. However, the accumulation of heat in the cutting zone would increase due to low thermal conductivity of these tools compared to carbide tools. These extreme conditions give rise to elevated friction levels and adhesion at the I_{CT} [43] and, thus, would facilitate the diffusion of atoms from the tool to the chips and vice-versa. In this regard, Fig. 15 shows the EDS spectrum of the magnified SEM micrographs at the I_{CT} for uncoated and coated cutting

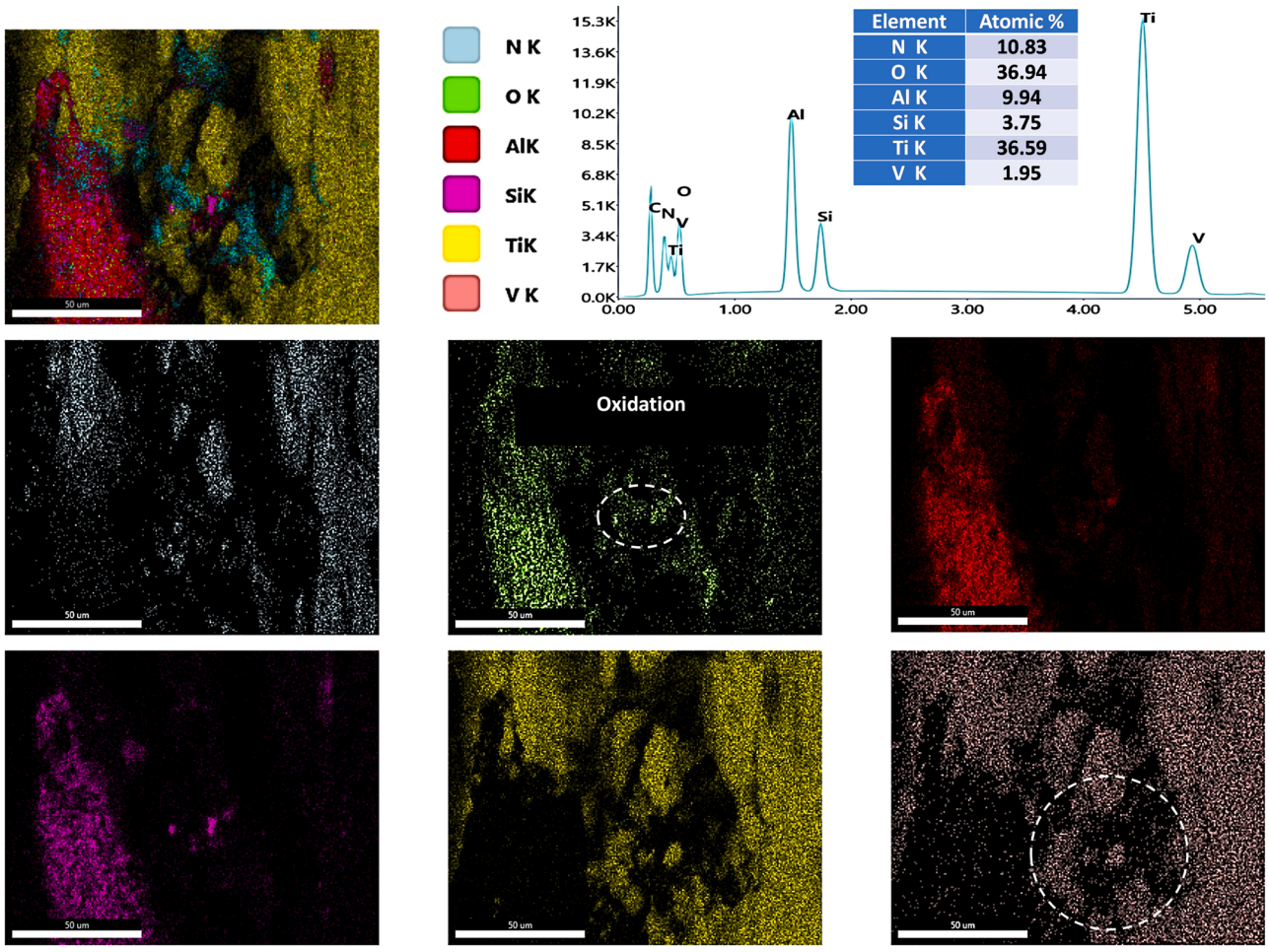

Fig. 13. EDS elemental mapping showing oxidation of vanadium in TiSiVN coated cutting tool.

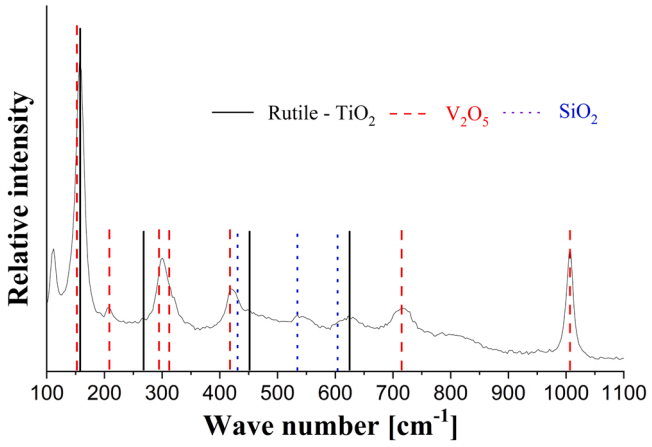

Fig. 14. Raman spectroscopy showing oxidation behaviour of TiSiVN coating.

tools at 125 m/min cutting speed. The EDS spectrum and the SEM images show that the chip movement causes material adhesion on the tool rake face. Also, the presence of Al for the coated tools on the I_{CT} indicates the removal of tool material due to erosion from the moving chips. However, it is not possible to confirm diffusion of tool material to the moving chips and thus, the machined surface of the chips has been investigated for possible diffusion of tool material (see Fig. 16). Al is evidently present on the machined surface of the chips which validates the diffusion process. Further, the coated tools especially with TiSiVN coating account to much lower diffusion which is obvious from the SEM micrographs. On the contrary, it is very difficult to predict the amount of diffusion on to the chips but an estimate can be made by plotting *Ti%* at the I_{CT} against cutting temperature (Fig. 17). The Ti adhesion on the I_{CT} increases with increase in temperature for uncoated and TiSiN coated tool. However, there is no noticeable change in *Ti%* with the increase of cutting temperature. Higher adhesion in combination with elevated cutting temperature would lead to more diffusion due to increase of friction at the I_{CT}. Thus, tool with TiSiVN coating would account to lower diffusion levels in comparison to uncoated and TiSiN coated tools.

4. Conclusions

The present investigation explores the chip-tool interface of Al_2O_3/SiC whiskers reinforced cutting tools during dry machining of Ti-6Al-4 V titanium alloy and studies the self-lubricating behaviour of TiSiVN coating during the machining operation. From the above work, the following conclusions can be drawn.

1. Lower surface roughness at the I_{CT} for TiSiN and TiSiVN coated tools than uncoated tools indicate superior anti-adhesive properties for the coatings. The increase of crater depth at some point causes loss of effective cutting edge for the uncoated tool and, thus, decreases *Ra* values at the highest cutting speed of 125 m/min for the uncoated tool.
2. The lower penetration of C_{HI} for TiSiN and TiSiVN coated tools compared to uncoated tools at higher cutting speeds exhibits

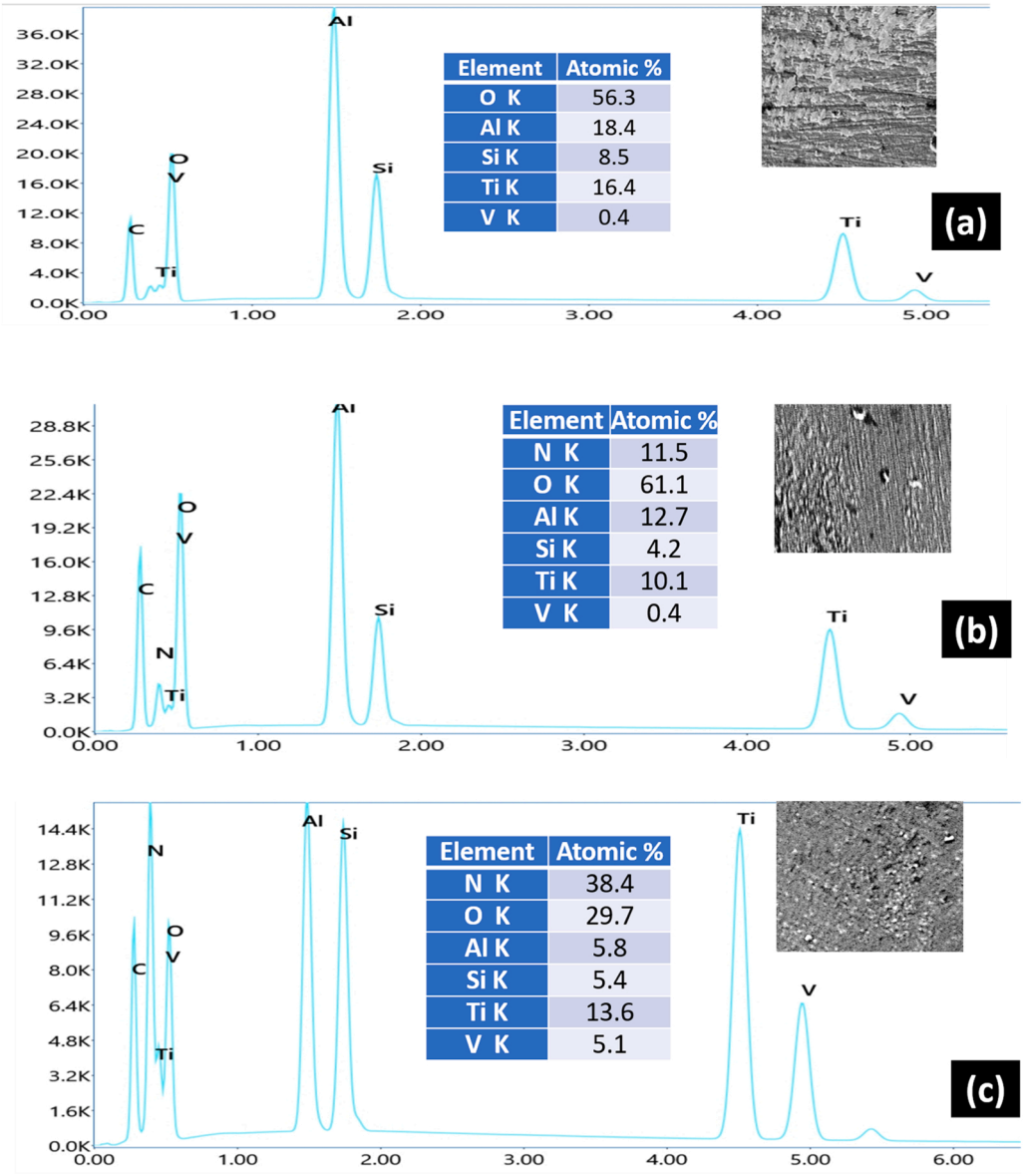

Fig. 15. EDS spectrum of the magnified SEM micrographs at the I_{CT} for (a) uncoated, (b) TiSiN coated, and (c) TiSiVN coated tools.

superior wear resistance for coatings, with TiSiVN coating outperforming the TiSiN coating mainly due to its self-lubricating properties.

3. The severe crater depth increments for the uncoated tool at higher cutting speeds in combination with high chip flow velocity due to the increase of cutting speed bends the chips away from the tool face resulting in lower adhesion at the I_{CT}. On the contrary, *AH* increases with increased cutting speed for both coated tools, indicating that the crater depth increment was not so severe for the coated tools. TiSiVN coated tool interestingly accounted to very low levels of *AH*. The *Ti%* on the I_{CT} follows the trend of *AH* variation with cutting speed for both uncoated and coated cutting tools. The TiSiVN coating accounts to a maximum reduction of approximately 23% in *AH* and 18% in *Ti %* when compared to the uncoated tool.
4. The variation of *AH* with cutting temperature clearly shows the dominant influence of cutting temperature on material adhesion at the I_{CT}. The TiSiVN coated tool exhibited low levels of adhesion and chip bending compared to TiSiN coated and uncoated tools, even at high cutting temperatures. A drastic upward surge of crater depth for uncoated and TiSiN coated tools at 125 m/min cutting speed makes the crater edge near the I_{CT} act as a chip breaker and facilitates the chip's bending away from the tool face causing reduction in chip bend angles.
5. The elemental mapping shows the presence of oxygen along with vanadium, which is an indication of vanadium oxidation that is a necessary condition for forming V-O oxides. These oxides form a tribolayer reducing friction at the I_{CT} and at sliding contact of the flank-workpiece interface, reducing erosion of the tool.
6. The wear on the I_{CT} is characterized by adhesion, abrasion and diffusion. The diffusion for TiSiVN coating would be inferior due to lower cutting temperatures, and self-lubrication offered by the formation of oxides of vanadium. Further, a 37% lesser O% at the highest cutting speed for TiSiVN coated tool when compared to the uncoated tool indicates reduced oxidation of the TiSiVN coating which is supported by lower levels of AH and cutting temperatures.

From the above results, it is evident that TiSiVN coating exhibits self-lubricating properties accounting to lower cutting temperatures, adhesion height, and roughness at the I_{CT}. The work provides a base for future investigation on the formation of tribolayer between the adhesion layer

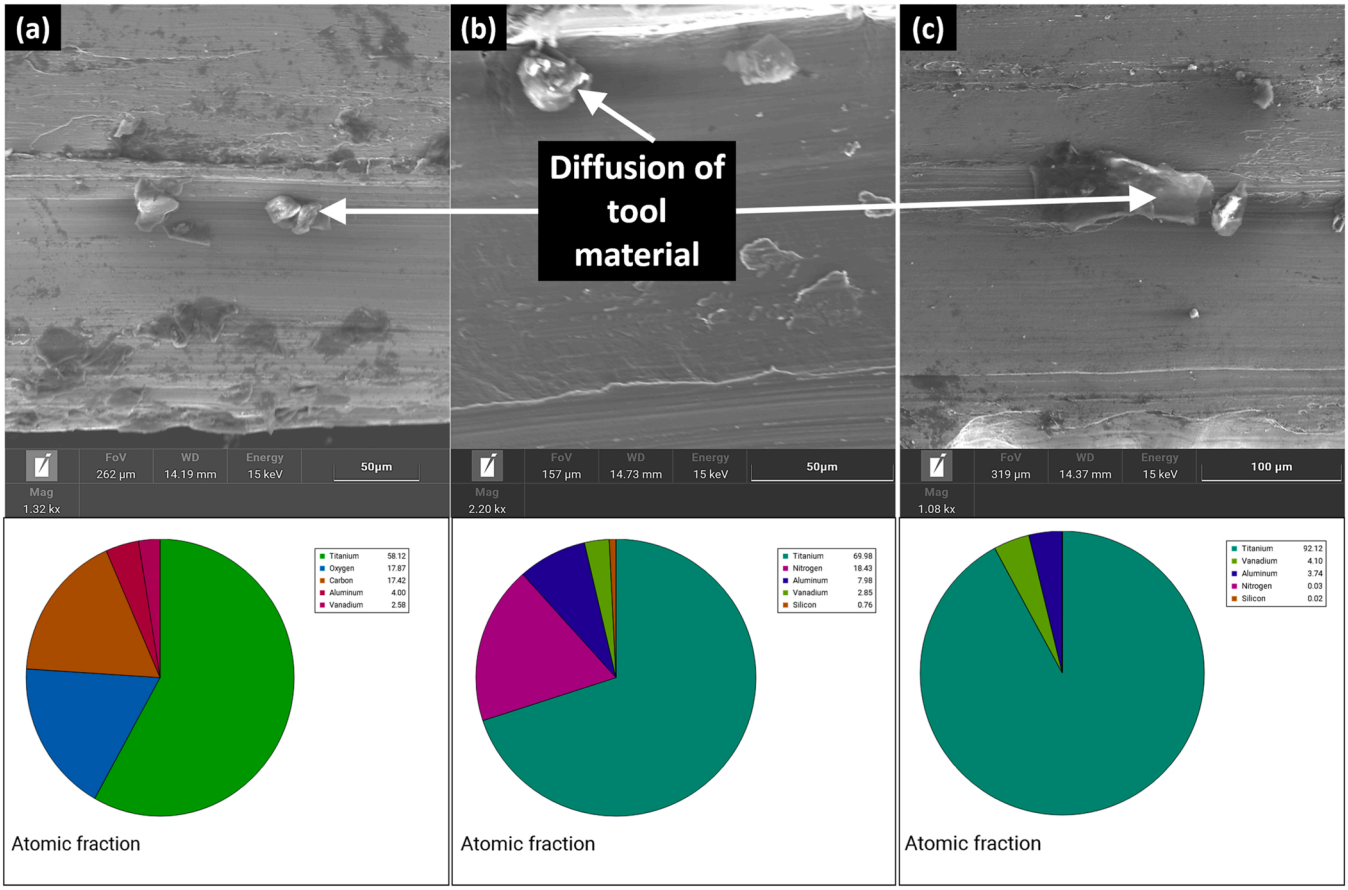

Fig. 16. Magnified SEM micrographs and EDS atomic fraction of chips formed while machining at 125 m/min cutting speed for (a) uncoated (b) TiSiN coated, and (c) TiSiVN coated Al_2O_3/SiC ceramic cutting tools.

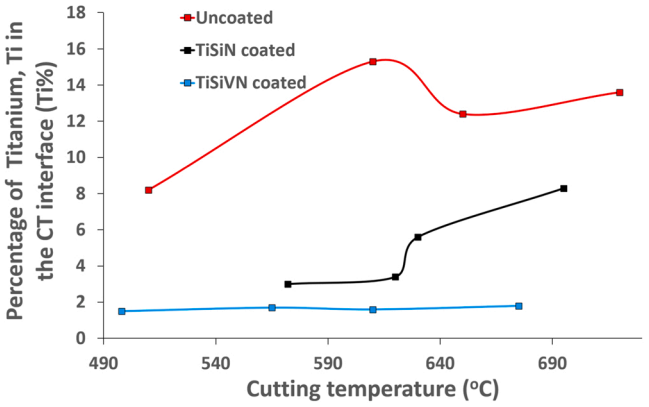

Fig. 17. *Ti%* variation with cutting temperature for uncoated and coated cutting tools.

and the top surface of the coating during machining with self-lubricant coatings. However, presence of vanadium in the workpiece material makes it difficult to quantify the thickness of tribolayer on the coating surface of TiSiVN. On the contrary, a good estimate of oxidation, workpiece adhesion, and diffusion has been provided by EDS analysis on the I_{CT} which is sufficient to support the performance enhancement offered by the TiSiVN coating. A transmission electron microscopy (TEM) analysis of the cross-section at the I_{CT} will be quite interesting to understand the diffusion of vanadium on the top surface during machining of materials without vanadium.

Declaration of Competing Interest

The authors declare that they have no known competing financial interests or personal relationships that could have appeared to influence the work reported in this paper.

Data Availability

The authors do not have permission to share data.

Acknowledgements

The work is supported by Maria Zambrano grants and funded by: MCIN/AEI/10.13039/501100011033 and "FSE invierte en tu futuro", and Basque Government university group IT1573-22, High performance machining, and MiCINN PDC2021–121792-I00 "New tooling production oriented to manufacture high value-added components of turbomachinery" (Haute Couture Taylor Made). The authors are also grateful to Grant PID2019-109340RB-I00 funded by MCIN/AEI/10.13039/5 The authors thank SGIker (UPV/EHU/ERDF, EU) for technical and human support provided. Also, Filipe Fernandes acknowledges the MCTool21 - ref. "POCI-01–0247- FEDER-045940" and CEMMPRE – ref. "UIDB/00285/2020″ projects, sponsored by FEDER funds through the COMPETE program – Operational Program on Competitiveness Factors – and by national funds through FCT – Foundation for Science and Technology.

References

[1] Özel T, Ulutan D. Prediction of machining induced residual stresses in turning of titanium and nickel based alloys with experiments and finite element simulations. CIRP Ann - Manuf Technol 2012;61:547–50. https://doi.org/10.1016/j.cirp.2012.03.100.

[2] Hosseini A, Kishawy HA. Mach Titan Alloy 2014. https://doi.org/10.1007/978-3-662-43902-9.

[3] Venugopal KA, Paul S, Chattopadhyay AB. Growth of tool wear in turning of Ti-6Al-4V alloy under cryogenic cooling. Wear 2007;262:1071–8. https://doi.org/10.1016/j.wear.2006.11.010.

[4] Hosseini A, Kishawy HA. Machining of Titanium Alloys. Berlin, Heidelberg: Springer Berlin Heidelberg; 2014. https://doi.org/10.1007/978-3-662-43902-9.

[5] da Silva LR, da Silva OS, dos Santos FV, Duarte FJ, Veloso GV. Wear mechanisms of cutting tools in high-speed turning of Ti6Al4V alloy. Int J Adv Manuf Technol 2019;103:37–48. https://doi.org/10.1007/s00170-019-03519-2.

[6] Jamil M, He N, Gupta MK, Zhao W, Khan AM. Tool wear mechanisms and its influence on machining tribology of face milled titanium alloy under sustainable hybrid lubri-cooling. Tribol Int 2022;170:107497. https://doi.org/10.1016/j.triboint.2022.107497.

[7] Lindvall R, Lenrick F, Persson H, M'Saoubi R, Ståhl JE, Bushlya V. Performance and wear mechanisms of PCD and pcBN cutting tools during machining titanium alloy Ti6Al4V. Wear 2020;454–455:203329. https://doi.org/10.1016/j.wear.2020.203329.

[8] Ko YM, Kwon WT, Kim YW. Development of Al2O3-SiC composite tool for machining application. Ceram Int 2004;30:2081–6. https://doi.org/10.1016/j.ceramint.2003.11.011.

[9] Sateesh Kumar C, Patel SKumar. Hard machining performance of PVD AlCrN coated Al2O3/TiCN ceramic inserts as a function of thin film thickness. Ceram Int 2017;43:13314–29. https://doi.org/10.1016/j.ceramint.2017.07.030.

[10] Das SR, Dhupal D, Kumar A. Experimental investigation into machinability of hardened AISI 4140 steel using TiN coated ceramic tool. Meas J Int Meas Confed 2015;62:108–26. https://doi.org/10.1016/j.measurement.2014.11.008.

[11] Chinchanikar S, Choudhury SK. Hard turning using HiPIMS-coated carbide tools: Wear behavior under dry and minimum quantity lubrication (MQL). Meas J Int Meas Confed 2014;55:536–48. https://doi.org/10.1016/j.measurement.2014.06.002.

[12] Chetan, Ghosh S, Rao PV. Environment friendly machining of Ni-Cr-Co based super alloy using different sustainable techniques. Mater Manuf Process 2016;31:852–9. https://doi.org/10.1080/10426914.2015.1037913.

[13] Salur E. Understandings the tribological mechanism of Inconel 718 alloy machined under different cooling/lubrication conditions. Tribol Int 2022;174:107677. https://doi.org/10.1016/j.triboint.2022.107677.

[14] Ross NS, Ganesh M, Srinivasan D, Gupta MK, Korkmaz ME, Krolczyk JB. Role of sustainable cooling/lubrication conditions in improving the tribological and machining characteristics of Monel-400 alloy. Tribol Int 2022;176:107880. https://doi.org/10.1016/j.triboint.2022.107880.

[15] Airao J, Khanna N, Nirala CK. Tool wear reduction in machining Inconel 718 by using novel sustainable cryo-lubrication techniques. Tribol Int 2022;175:107813. https://doi.org/10.1016/j.triboint.2022.107813.

[16] Singh R, Dureja JS, Dogra M, Gupta MK, Mia M, Song Q. Wear behavior of textured tools under graphene-assisted minimum quantity lubrication system in machining Ti-6Al-4V alloy. Tribol Int 2020;145:106183. https://doi.org/10.1016/j.triboint.2020.106183.

[17] Gupta MK, Song Q, Liu Z, Sarikaya M, Jamil M, Mia M, et al. Experimental characterisation of the performance of hybrid cryo-lubrication assisted turning of Ti–6Al–4V alloy. Tribol Int 2021;153. https://doi.org/10.1016/j.triboint.2020.106582.

[18] Eltaggaz A, Nouzil I, Deiab I. Machining ti-6al-4v alloy using nano-cutting fluids: investigation and analysis. J Manuf Mater Process 2021;5. https://doi.org/10.3390/jmmp5020042.

[19] Shokrani A, Dhokia V, Newman ST. Hybrid cooling and lubricating technology for CNC milling of inconel 718 nickel alloy. Procedia Manuf 2017;11:625–32. https://doi.org/10.1016/j.promfg.2017.07.160.

[20] Jamil M, Zhao W, He N, Gupta MK, Sarikaya M, Khan AM, et al. Sustainable milling of Ti–6Al–4V: a trade-off between energy efficiency, carbon emissions and machining characteristics under MQL and cryogenic environment. J Clean Prod 2021;281:125374. https://doi.org/10.1016/j.jclepro.2020.125374.

[21] Krolczyk GM, Maruda RW, Krolczyk JB, Wojciechowski S, Mia M, Nieslony P, et al. Ecological trends in machining as a key factor in sustainable production – a review. J Clean Prod 2019;218:601–15. https://doi.org/10.1016/j.jclepro.2019.02.017.

[22] Uhlmann E, Oyanedel Fuentes JA, Gerstenberger R, Frank H. Nc-AlTiN/a-Si3N4 and nc-AlCrN/a-Si3N4 nanocomposite coatings as protection layer for PCBN tools in hard machining. Surf Coat Technol 2013;237:142–8. https://doi.org/10.1016/j.surfcoat.2013.09.017.

[23] More AS, Jiang W, Brown WD, Malshe AP. Tool wear and machining performance of cBN-TiN coated carbide inserts and PCBN compact inserts in turning AISI 4340 hardened steel. J Mater Process Technol 2006;180:253–62. https://doi.org/10.1016/j.jmatprotec.2006.06.013.

[24] Strano M, Albertelli P, Chiappini E, Tirelli S. Wear behaviour of PVD coated and cryogenically treated tools for Ti-6Al-4V turning. Int J Mater Form 2015;8:601–11. https://doi.org/10.1007/s12289-014-1215-6.

[25] Sateesh Kumar C, Majumder H, Khan A, Patel SK. Applicability of DLC and WC/C low friction coatings on Al2O3/TiCN mixed ceramic cutting tools for dry machining of hardened 52100 steel. Ceram Int 2020;46:11889–97. https://doi.org/10.1016/j.ceramint.2020.01.225.

[26] Kalss W, Reiter A, Derflinger V, Gey C, Endrino JL. Modern coatings in high performance cutting applications. Int J Refract Met Hard Mater 2006;24:399–404. https://doi.org/10.1016/j.ijrmhm.2005.11.005.

[27] Vereschaka AA, Grigoriev SN, Vereschaka AS, Popov AY, Batako AD. Nano-scale multilayered composite coatings for cutting tools operating under heavy cutting conditions. Procedia CIRP 2014;14:239–44. https://doi.org/10.1016/j.procir.2014.03.070.

[28] Işıldak YE, Ergüder TO, Kaya G, Hacısalihoğlu İ, Yay B, Yıldız F. Wear behavior of Ni-B coated-hard anodized Al7Si alloy and machining performance with ZrN ceramic film coated carbide tool. Surf Interfaces 2020;21:100768. https://doi.org/10.1016/j.surfin.2020.100768.

[29] Cavaleiro D, Figueiredo D, Moura CW, Cavaleiro A, Carvalho S. Machining performance of TiSiN (Ag) coated tools during dry turning of TiAl6V4 aerospace alloy. Ceram Int 2021;47:11799–806. https://doi.org/10.1016/j.ceramint.2021.01.021.

[30] Franz R, Mitterer C. Vanadium containing self-adaptive low-friction hard coatings for high-temperature applications: a review. Surf Coat Technol 2013;228:1–13. https://doi.org/10.1016/j.surfcoat.2013.04.034.

[31] Fernandes F, Oliveira JC, Cavaleiro A. Self-lubricating TiSi(V)N thin films deposited by deep oscillation magnetron sputtering (DOMS). Surf Coat Technol 2016;308:256–63. https://doi.org/10.1016/j.surfcoat.2016.07.039.

[32] Molaiekiya F, Aramesh M, Veldhuis SC. Chip formation and tribological behavior in high-speed milling of IN718 with ceramic tools. Wear 2020:446–7. https://doi.org/10.1016/j.wear.2020.203191.

[33] Gekonde HO, Subramanian SV. Tribology of tool – chip interface and tool wear mechanisms. Surf Coat Technol 2002;149:151–60. https://doi.org/10.1016/S0257-8972(01)01488-8.

[34] Lu J, Chen J, Fang Q, Liu B, Liu Y, Jin T. Finite element simulation for Ti-6Al-4V alloy deformation near the exit of orthogonal cutting. Int J Adv Manuf Technol 2016;85:2377–88. https://doi.org/10.1007/s00170-015-8077-z.

[35] Kumar CS, Patel SK. Effect of chip sliding velocity and temperature on the wear behaviour of PVD AlCrN and AlTiN coated mixed alumina cutting tools during turning of hardened steel. Surf Coat Technol 2017;334:509–25. https://doi.org/10.1016/j.surfcoat.2017.12.013.

[36] Da Silva MB, Wallbank J. Cutting temperature: prediction and measurement methods - a review. J Mater Process Technol 1999;88:195–202. https://doi.org/10.1016/S0924-0136(98)00395-1.

[37] Wagner V, Baili M, Dessein G. The relationship between the cutting speed, tool wear, and chip formation during Ti-5553 dry cutting. Int J Adv Manuf Technol 2015;76:893–912. https://doi.org/10.1007/s00170-014-6326-1.

[38] Kumar CS, Patel SK. Performance analysis and comparative assessment of nano-composite TiAlSiN/TiSiN/TiAlN coating in hard turning of AISI 52100 steel. Surf Coat Technol 2018;335:265–79. https://doi.org/10.1016/j.surfcoat.2017.12.048.

[39] Fernandes F, Loureiro A, Polcar T, Cavaleiro A. The effect of increasing V content on the structure, mechanical properties and oxidation resistance of Ti–Si–V–N films deposited by DC reactive magnetron sputtering. Appl Surf Sci 2014;289:114–23. https://doi.org/10.1016/j.apsusc.2013.10.117.

[40] Fernandes F, Morgiel J, Polcar T, Cavaleiro A. Oxidation and diffusion processes during annealing of TiSi(V)N films. Surf Coat Technol 2015;275:120–6. https://doi.org/10.1016/j.surfcoat.2015.05.031.

[41] Grearson AN. Evaluation of principal vvear mechanisms of carbides and ceramics used for machining. Mater Sci Technol 1986;2:47–58.

[42] Kumar CS, Patel SK. Experimental and numerical investigations on the effect of varying AlTiN coating thickness on hard machining performance of Al 2 O 3 -TiCN mixed ceramic inserts. Surf Coat Technol 2017;309:266–81. https://doi.org/10.1016/j.surfcoat.2016.11.080.

[43] Nouari M, Ginting A. Wear characteristics and performance of multi-layer CVD-coated alloyed carbide tool in dry end milling of titanium alloy. Surf Coat Technol 2006;200:5663–76. https://doi.org/10.1016/j.surfcoat.2005.07.063.